JOURNAL OF VIROLOGY, July 1997, p. 5012–5024 Vol. 71, No. 7
0022-538X/97/$04.00+0

Herpes Simplex Virus Type 1 Glycoprotein K Is Not Essential for Infectious Virus Production in Actively Replicating Cells but Is Required for Efficient Envelopment and Translocation of Infectious Virions from the Cytoplasm to the Extracellular Space

SUKHANYA JAYACHANDRA, ABOLGHASEM BAGHIAN, AND KONSTANTIN G. KOUSOULAS*

Department of Veterinary Microbiology and Parasitology, School of Veterinary Medicine, Louisiana State University, Baton Rouge, Louisiana 70803

Received 22 November 1996/Accepted 3 April 1997

We characterized the glycoprotein K (gK)-null herpes simplex virus type 1 [HSV-1] (KOS) ΔgK and compared it to the gK-null virus HSV-1 F-gKβ (L. Hutchinson et al., J. Virol. 69:5401–5413, 1995). ΔgK and F-gKβ mutant viruses produced small plaques on Vero cell monolayers at 48 h postinfection. F-gKβ caused extensive fusion of 143TK cells that was sensitive to melittin, a specific inhibitor of gK-induced cell fusion, while ΔgK virus did not fuse 143TK cells. A recombinant plasmid containing the truncated gK gene specified by F-gKβ failed to rescue the ICP27-null virus KOS (*d*27-1), while a plasmid with the ΔgK deletion rescued the *d*27-1 virus efficiently. ΔgK virus yield was approximately 100,000-fold lower in stationary cells than in actively replicating Vero cells. The plaquing efficiencies of ΔgK and F-gKβ virus stocks on VK302 cells were similar, while the plaquing efficiency of F-gKβ virus stocks on Vero cells was reduced nearly 10,000-fold in comparison to that of ΔgK virus. Mutant ΔgK and F-gKβ infectious virions accumulated within Vero and HEp-2 cells but failed to translocate to extracellular spaces. ΔgK capsids accumulated in the nuclei of Vero but not HEp-2 cells. Enveloped ΔgK virions were visualized in the cytoplasms of both Vero and HEp-2 cells, and viral capsids were found in the cytoplasm of HEp-2 cells within vesicles. Glycoproteins B, C, D, and H were expressed on the surface of ΔgK-infected Vero cells in amounts similar to those for KOS-infected Vero cells. These results indicate that gK is involved in nucleocapsid envelopment, and more importantly in the translocation of infectious virions from the cytoplasm to the extracellular spaces, and that actively replicating cells can partially compensate for the envelopment but not for the cellular egress deficiency of the ΔgK virus. Comparison of ΔgK and F-gKβ viruses suggests that the inefficient viral replication and plaquing efficiency of F-gKβ virus in Vero cells and its syncytial phenotype in 143TK$^-$ cells are most likely due to expression of a truncated gK.

HSV-1 membrane fusion. Herpes simplex virus type 1 (HSV-1) entry, nucleocapsid envelopment, egress, and transfer of infectious virions from infected to uninfected cells involve fusion of cellular and viral membranes that are thought to be regulated by membrane-associated virus-specified proteins and glycoproteins (46, 52). Syncytial mutations that cause extensive virus-induced cell fusion can arise in at least four different regions of the viral genome, including the UL20 gene (6, 35); the UL24 gene (30, 49); the UL27 gene, encoding glycoprotein B (gB) (13, 41); and the UL53 gene, coding for glycoprotein K (gK) (8, 22, 42, 48). Syncytial mutations in UL53 (gK) gene are more frequently isolated than syncytial mutations in any other genes (8, 9, 22, 24, 42–44, 48). Studies with anti-gK serum raised against peptides that represented immunogenic portions of gK detected the glycoprotein in the nuclear and perinuclear space, but not in the plasma membrane, of infected cells. Furthermore, based on studies with these antipeptide sera, it is believed that gK is not part of the viral envelope (27, 29).

HSV-1 nucleocapsid envelopment and cellular egress. Herpesvirus capsids acquire their envelope by budding through the inner lamellae of the nuclear membrane (20, 38, 50). The release of infectious virions from infected cells requires the transport of infectious virions from the perinuclear to the extracellular space. This translocation most likely occurs within transport vesicles derived from the outer lamellae of the nuclear membrane and the contiguous endoplasmic reticulum (ER) (14, 20, 21, 38, 50; reviewed in reference 46). An alternative model that involves de-envelopment at the outer nuclear membrane followed by envelopment at the rough ER (RER) and/or the Golgi complex has also been proposed (39, 40, 46, 53, 56). Golgi-dependent glycoprotein maturation is vital for cellular egress, because in cells defective in the processing of high-mannose precursor glycoproteins to mature glycoproteins, or when Golgi-dependent functions are inhibited by the ionophore monensin, infectious virions accumulate in the cytoplasm but are not transported into the extracellular space (7, 16, 31). HSV specifies at least three viral proteins which are involved in the transport of enveloped virions to extracellular spaces. The UL20 protein seems to be involved in a postenvelopment virion transport step, because UL20-null mutant viruses envelope in the inner lamellae of the nuclear membranes but are retained within the perinuclear space of Vero cells. However, certain other cells are able to complement the UL20-null defect and allow UL20-null virions to overcome this early block in the translocation pathway, indicating that cellular factors are involved (1, 6, 35, 54). Glycoprotein H (gH) may play an important role in cellular egress of

* Corresponding author. Phone: (504) 346-3312.

infectious virions, because temperature-sensitive mutant viruses with mutated gH are retained within cells, while virions that lack gH are released by infected cells (23). Furthermore, targeting gH to the RER with the specific retention motif KKXX results in virions released by infected cells that are not infectious, while infectious virions that contain gH are retained in the cytoplasm (11). Glycoprotein D (gD) may also affect intracellular virion transport, because HSV-1 gD mutants that overcome gD-mediated interference de-envelope in gD-expressing cells (14).

To characterize the role of gK in virus replication and membrane fusion, we constructed and characterized the HSV-1 mutant virus ΔgK, which lacks the entire UL53 (gK) gene. ΔgK virus is genotypically and phenotypically different from the previously reported F-gKβ mutant virus. F-gKβ was generated by insertion of an ICP6::*lacZ* cassette into the *Hpa*I site 336 nucleotides from the start of the UL53 open reading frame (ORF), allowing expression of the amino-terminal one-third of the gK polypeptide (28). The F-gKβ plaquing efficiency on log-phase Vero cells was reduced 1,000- to 10,000-fold in comparison to that of ΔgK. Furthermore, F-gKβ caused extensive fusion of 143TK$^-$ cells which was inhibited by melittin, while ΔgK did not cause any virus-induced cell fusion. A recombinant plasmid carrying the F-gKβ truncated gene failed to rescue the KOS (*d*27-1) mutant virus, while a similar plasmid containing the ΔgK deletion in gK rescued the *d*27-1 virus efficiently. Our results indicate that gK is required for efficient virus envelopment and translocation of infectious virions to extracellular, cell-free spaces, and they suggest that the observed phenotypic properties of F-gKβ are due to expression of the amino-terminal portion of gK.

MATERIALS AND METHODS

Cell and viruses. African green monkey kidney (Vero), human epidermoid larynx carcinoma (HEp-2), and rabbit skin cells were obtained from the American Type Culture Collection (Rockville, Md.). Cells were propagated and maintained in Dulbecco's modified Eagle's medium (DMEM; Sigma Chemical Co., St. Louis, Mo.) supplemented with 10% heat-inactivated fetal bovine serum (FBS). V27 cells carry a stably integrated copy of the HSV-1 (KOS) ICP27 gene, kindly provided by D. M. Knipe, Harvard Medical School. These cells were propagated in DMEM supplemented with 10% FBS (45). VK302, a gK-transformed cell line, was obtained from D. C. Johnson, Oregon Health Sciences University, and maintained in DMEM lacking histidine (GIBCO Laboratories, Grand Island, N.Y.) supplemented with 10% FBS and 0.3 mM histidinol (Sigma). All cells were passaged once in DMEM plus 10% FBS without selection prior to infection with virus (28). HSV-1 (KOS), the parental wild-type strain used in this study, was originally obtained from P. A. Schaffer (Dana-Farber Cancer Institute, Boston, Mass.). HSV-1 (KOS) *d*27-1, which has a 1.6-kb *Bam*HI-*Stu*I deletion of the ICP27 gene, was kindly provided by D. M. Knipe and was propagated in V27 cells (45). The gK mutant F-gKβ was a kind gift from D. C. Johnson and was propagated in VK302 cells (28). HSV-1 mp (MP) was obtained from B. Roizman, University of Chicago, Chicago, Ill.

Reagents. Restriction enzymes, DNA modification enzymes, and the SpeI* linker were obtained from New England Biolabs (Beverly, Mass.). Deoxynucleotide triphosphates, sequencing buffers, and T7 Sequenase were obtained from United States Biochemical Corp. (Cleveland, Ohio) and were used in the dideoxy-chain termination method as instructed by the manufacturer. Monoclonal antibody (MAb) HS-B1 against gB, MAb HS-C1 against gC, and mouse monospecific polyclonal antisera against gD were produced in our laboratory by following standard procedures (3, 5). MAb 52-S against gH was obtained from the American Type Culture Collection (ATCC). Melittin was purchased from Sigma and used as described previously (4). [^{35}S]methionine (13.62 mCi/ml) was from ICN Radiochemicals (Irvine, Calif.), and [^{35}S]dATP (sequencing grade; 12.5 mCi/ml) was from DuPont/NEN (Wilmington, Del.).

Plasmids. Plasmid pSG28, containing the *Eco*RI E through K fragments of HSV-1 (KOS) inserted into pBR325, was a gift from R. M. Sandri-Goldin (University of California, Irvine) and was described previously (25). The 3.2-kbp *Eco*RI-*Bam*HI fragment, which contains the carboxy-terminal two-thirds of the UL52 ORF and the complete UL53 ORF, was removed from pSG28 and was inserted into the multiple cloning site of plasmid pUC19 to generate plasmid pSJ1710. Plasmid pSJ1711, derived from pSJ1710, contains an *Spe*I* linker (CT AGACTAGTCTAG; carries stop codons in all three reading frames and the recognition sequence for restriction enzyme *Spe*I) at the unique *Bbs*I site (within the UL53 ORF at nucleotide 75 from the start codon). A plasmid that contains the HSV-1 (KOS) *Bam*HI B fragment in pUC19 was kindly provided by Bill Goins (University of Pittsburgh). Plasmid pSJ1722 was derived from *Bam*HI-B by excising the *Bam*HI-*Pst*I fragment that contains the HSV-1 (KOS) UL54 ORF (coding for ICP27) and cloning it into the multiple cloning site of pUC19. Plasmid pSJ1723 was derived by removing the *Bam*HI-*Hin*dIII fragment from pSJ1722 and inserting it into *Bam*HI-*Hin*dIII site of pSJ1711 in such a way as to reassemble the UL52, UL53, and UL54 ORFs in sequence. Finally, plasmid pSJ1724 was derived by eliminating a 1-kbp *Spe*I-*Bam*HI fragment from pSJ1723 that deleted the entire UL53 ORF but kept the UL52 and UL54 ORFs intact. Plasmid pSJ1763 was constructed by inserting a 618-bp F-gKβ DNA fragment into plasmid pSJ1723, using restrictions sites *Kpn*I and *Bam*HI. This 618-bp DNA fragment was amplified by PCR from purified F-gKβ viral DNA by using synthetic oligonucleotide primers P2 (5′-TGGGTCCTCCTACAGCTA-3′) and P5 (5′-GGGGAGCTGGATCCTGATCACGTACA-3′) and is demarcated by a *Kpn*I restriction site upstream of the gK gene at the 5′ end and a synthetic *Bam*HI site inserted immediately after the stop codon which terminates the truncated gK.

Construction of the ΔgK mutant virus. Rabbit skin cells were transfected with plasmid pSJ1724 by the calcium chloride precipitation method (18), and 18 h posttransfection, cells were infected with *d*27-1 (ICP27-null) virus; 24 h postinfection (hpi), the cells were lysed and virus stocks were made. Viral recombinants were grown on Vero cells. Twenty-five plaques were picked and plaque purified five times on Vero cells.

Rescue of the ΔgK mutant virus. Primers P1 and P4 (Fig. 1b) were used to generate the 3.9-kbp PCR fragment, using wild-type KOS viral DNA as the template. Vero cells were transfected with the wild-type KOS fragment by the calcium chloride precipitation method (18), and 24 h posttransfection, cells were infected with ΔgK virus. Cell cultures were incubated at 37°C for an additional 48 h, at which point virus stocks were prepared. Recombinant virus stocks were plated on subconfluent Vero cell monolayers (8×10^5 cells per 9.62 cm^2 at the time of infection) at different dilutions and allowed to replicate for 48 h. Large wild-type plaques were picked and plaque purified three times. These viruses were designated ΔgK1$^+$, ΔgK2$^+$, and ΔgK3$^+$.

Rescue of the *d*27-1 virus by plasmids pSJ1724 and pSJ1763, carrying the ΔgK and F-gKβ gene deletions, respectively. Rescue of the *d*27-1 virus was performed as described above for the construction of the ΔgK virus with the exception that Vero cell cultures were transfected with each plasmid separately and superinfected with *d*27-1 virus at a multiplicity of infection (MOI) of 10. Virus stocks were collected at 24 hpi, and titers were determined on Vero and VK302 cells. Twenty-five virus plaques from Vero cells were collected under agarose overlay, and infectious virions from each virus plaque were purified two times. Individual plaque-purified virus stocks were used to infect Vero cells for the purification of viral DNA.

Viral DNA. Viral DNA was prepared in Vero cells as described previously (33). Briefly, Vero cells were infected with plaque-purified virus at an MOI of 5. At 3 days postinfection, cells were lysed with 1% Nonidet P-40–0.5% deoxycholate in 10 mM Tris–1 mM EDTA. Lysates were treated with RNase (100 μg/ml) for 10 min at 37°C, followed by addition of 1% sodium dodecyl sulfate and proteinase K (100 μg/ml) for treatment at 55°C overnight. DNA was purified with two phenol ether extractions and precipitated with 3 M sodium acetate and ice-cold ethanol. To obtain ultrapure viral DNA, further purification through two NaI gradients was performed (33).

PCR detection of ΔgK and F-gKβ viruses. PCR was performed by using an XL PCR kit (Perkin-Elmer) as described previously (19). Viral DNA was prepared as described earlier. Approximately 100 ng of viral DNA was used in a total reaction volume of 100 μl. PCR primers were P1 (5′-GGCAACGACGACGG GGACTGGT-3′), P2 (5′-TGGGTCCTCCTACAGCTA), P3 (5′-GGCACAGA CAAGGACCAATCAGACACCA-3′), and P4 (5′-TCTCTCCGACCCCGACA CCAA-3′) (Fig. 1b). All of the primers were synthesized in our laboratory on Perkin-Elmer/Applied Biosystems DNA synthesizer model 394, using phosphoramidite chemistry. The XL-PCR reaction conditions were as follows: 94°C for 5 s and 68°C for 8 min for 30 cycles.

Southern blot analysis of viral DNA. DNA from either KOS- or ΔgK-infected Vero cells was extracted as described previously (17). The purified DNA was digested with restriction endonuclease *Bam*HI (New England Biolabs), electrophoresed on a 0.8% agarose gel, transferred by the Southern blot method (51) to positively charged nylon membranes, and hybridized with a biotin-labeled probe. The probe was derived from a 3.2-kbp PCR fragment which contains portions of the UL52 ORF, the complete UL53 ORF, and a portion of the UL54 ORF. This PCR fragment was purified and labeled with biotin-dUTP by using a NEBlot phototope kit (New England Biolabs), which incorporates biotin into the probe through a random primer reaction. Prehybridization, hybridization, and detection of the biotinylated probe were achieved by using the Southern-Light chemiluminescent detection system as instructed by the manufacturer (Tropix, Inc., Bedford, Mass.).

Visualization of intracellular virus particles in Vero and HEp-2 cells by electron microscopy. Vero and HEp-2 cells were infected with ΔgK or wild-type KOS virus at an MOI of 10 and were incubated at 37°C for 24 to 48 h. The infected cells were washed three times with 1× phosphate-buffered saline and fixed with 2% glutaraldehyde in 0.1 M sodium cacodylate (CAC) buffer (pH 7.4) for 1 h at room temperature. Cells were then washed three times with 0.1 M CAC

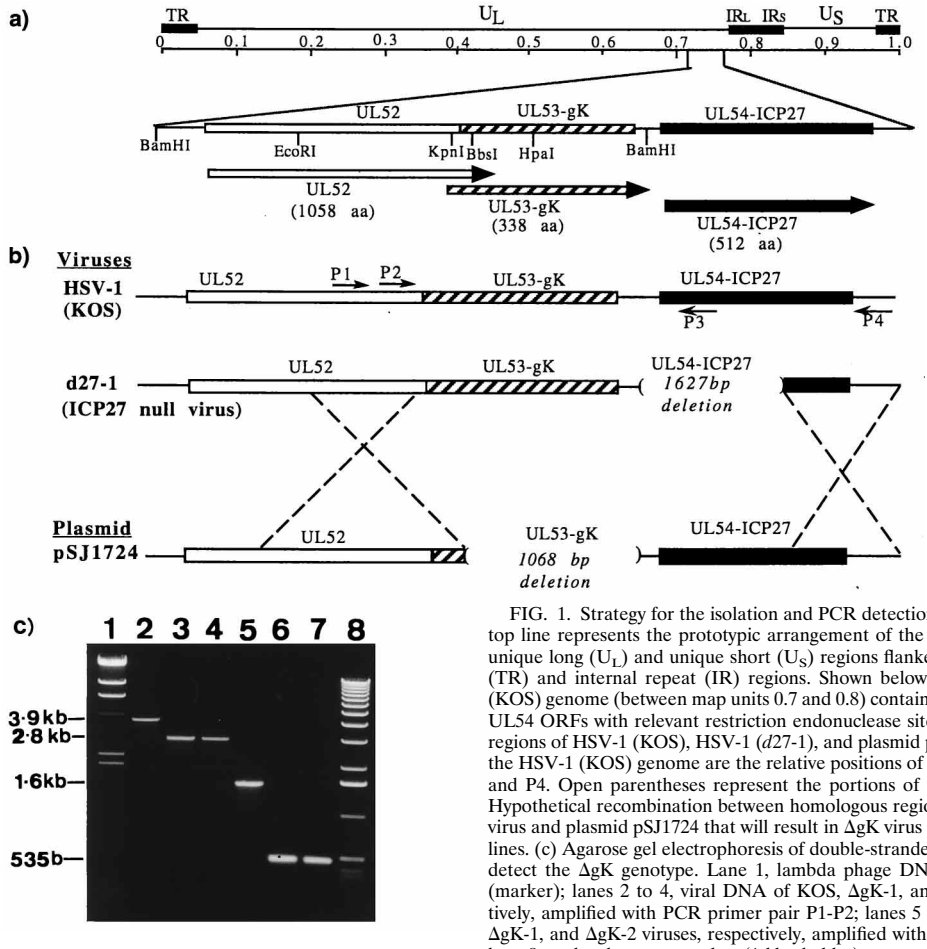

FIG. 1. Strategy for the isolation and PCR detection of HSV-1 ΔgK. (a) The top line represents the prototypic arrangement of the HSV-1 genome with the unique long (U_L) and unique short (U_S) regions flanked by the terminal repeat (TR) and internal repeat (IR) regions. Shown below is the region of HSV-1 (KOS) genome (between map units 0.7 and 0.8) containing the UL52, UL53, and UL54 ORFs with relevant restriction endonuclease sites. (b) Relevant genomic regions of HSV-1 (KOS), HSV-1 (*d*27-1), and plasmid pSJ1724. Represented on the HSV-1 (KOS) genome are the relative positions of PCR primers, P1, P2, P3, and P4. Open parentheses represent the portions of genes that were deleted. Hypothetical recombination between homologous regions of *d*27-1 (ICP27-null) virus and plasmid pSJ1724 that will result in ΔgK virus is depicted by the dashed lines. (c) Agarose gel electrophoresis of double-stranded DNA PCR products to detect the ΔgK genotype. Lane 1, lambda phage DNA digested with *Hin*dIII (marker); lanes 2 to 4, viral DNA of KOS, ΔgK-1, and ΔgK-2 viruses, respectively, amplified with PCR primer pair P1-P2; lanes 5 to 7, viral DNA of KOS, ΔgK-1, and ΔgK-2 viruses, respectively, amplified with PCR primer pair P3-P4; lane 8, molecular mass marker (1-kbp ladder).

buffer supplemented with 5% sucrose (pH 7.4) at room temperature and fixed with a 1% osmium tetroxide–1% potassium ferrocyanide solution for 1.5 h. Cells were further washed three times at room temperature with 5% sucrose in 0.1 M CAC buffer, stained with 2.5% uranyl acetate in distilled water, and refrigerated overnight. Finally cells were washed in distilled water, dehydrated by using gradient steps of ethanol, filtrated with Epon-araldite resin, and polymerized for 24 h at 60°C. Sample blocks were sectioned and mounted on grids, and at least five sections and 10 different infected cells per section were examined in a Philips 410 electron microscope for the presence of viral particles (17).

Kinetics of infectious virus production. Subconfluent Vero and HEp-2 cell monolayers containing approximately 8×10^5 cells per 9.62-cm^2 well at the time of infection were infected with either ΔgK, F-gKβ, KOS, or ΔgK^+ virus at an MOI of 10. After a 60-min adsorption at 4°C, viruses were removed and cultures were washed with medium. Fresh prewarmed medium was added to the cells, and cultures were incubated at 37°C for the duration of the study. At selected times, the supernatants and the cell pellets were harvested and collected in separate tubes. The samples were frozen and thawed three times and sonicated, and standard endpoint plaque assays were carried out on Vero cells.

Cell staining and fluorescence cytometry. Relative levels of individual glycoproteins on the surface of KOS- and ΔgK-infected Vero cells were determined essentially as described previously (2). Briefly, subconfluent Vero cell monolayers were infected with either KOS or ΔgK virus at an MOI of 5, and cells were harvested by mild trypsinization at 6 hpi, labeled with MAbs to gB, gC, gD, and gH, and subsequently labeled with goat anti-mouse immunoglobulin G-fluorescein isothiocynate (FITC). The relative amounts of each glycoprotein on the surface of infected KOS and ΔgK Vero cells were detected by using a FACScan flow cytometer equipped with a 15-mW air-cooled 488-nm argon ion laser. The green fluorescence of FITC staining was collected with a 530/30-nm band pass filter. All samples were acquired and analyzed on a Hewlett-Packard (San Diego, Calif.) 340 computer, and the data were illustrated in the form of log green-fluorescence histograms by using the Lysys II software package (Becton Dickinson, San Jose, Calif.).

RESULTS

Construction of HSV-1 (KOS) ΔgK. HSV-1 (KOS) *d*27-1 is a host range mutant virus which carries a deletion in the ICP27-UL54 gene rendering the virus unable to replicate in Vero cells; however, infectious virions can be produced by complementation in the V27 cell line, which is permanently transformed with the ICP27 gene (45). Plasmid pSJ1724 was constructed to have a deletion of the entire portion of the gK gene that specifies the mature gK (see Materials and Methods). pSJ1724 was transfected into rabbit skin cells, and 24 h posttransfection, the cell cultures were infected with virus *d*27-1. Progeny recombinant viruses were expected to be generated in which the deletion in the ICP27 gene of the *d*27-1 genome was rescued by the intact ICP27 gene on the plasmid pSJ1724 as a result of homologous recombination between the *d*27-1 viral genome and the transfected plasmid pSJ1724 (Fig. 1b). ICP27 rescue could occur only if the gK deletion was also transferred into the recombinant viral genomes, because there were no homologous sequences between the gK and ICP27 genes that could be used to independently rescue the ICP27 gene deletion (Fig. 1b).

Putative recombinant virus stocks were plated on exponentially growing Vero cells, plaque purified at least five times, and genotyped by PCR and Southern blot assays. Different sets of PCR primers were designed to detect either the gK-null or

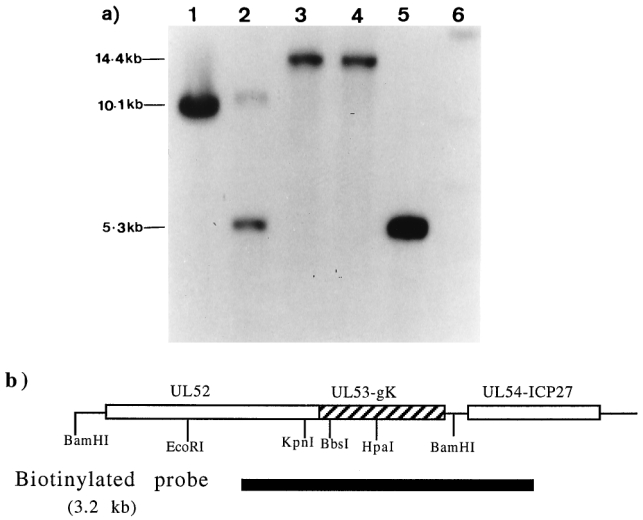

FIG. 2. Southern blot analysis of KOS and ΔgK viral DNAs. Lanes 1 and 5, plasmids pBamH I-B and pRB126 digested with *Bam*HI. Digestion of these plasmids with *Bam*HI results in the *Bam*HI B (10.1-kb) and L (5.3-kb) fragments, respectively. Lanes 2 to 4, KOS, ΔgK-1, and ΔgK-2 viral DNAs digested with restriction endonuclease *Bam*HI. Lane 6, lambda phage DNA digested with restriction enzyme, *Hin*dIII. (b) Location of the 3.2-kbp biotinylated probe relative to the viral genome.

ICP27-null genotype. Primers P1 and P2 were located within the UL52 coding sequence, whereas primers P3 and P4 were located within the UL54-ICP27 coding sequence (Fig. 1b). Primer P3 was located within the portion of UL54-ICP27 that was deleted, while primer P4 was located outside the deleted region (Fig. 1b). Primer pairs P1-P4 and P2-P3 amplified DNA fragments of 3,936 and 1,604 bp, respectively, when wild-type KOS was used as the control template DNA (Fig. 1c, lanes 2 and 5). Primer pairs P1-P4 and P2-P3 amplified DNA fragments of 2,868 bp (Fig. 1c, lanes 3 and 4) and 535 bp (Fig. 1c, lanes 6 and 7), respectively, from the recombinant viral stocks, indicating that these viral genomes contained the expected deletion of the gK gene, while no contaminating ICP27-null (*d*27-1) genotypes were detected (Fig. 1c). Six such viral isolates obtained from well-isolated and plaque-purified viral stocks were shown to contain exclusively gK-null viruses. These virus isolates were designated ΔgK-1 through -6.

The genotype of representative gK-null viruses, ΔgK-1 and ΔgK-2, was confirmed by Southern blotting (Fig. 2a). Viral DNAs from KOS and ΔgK were digested with restriction endonuclease *Bam*HI, separated by agarose gel electrophoresis, and transferred to a nylon membrane. The membrane was probed with a 3.2-kbp biotinylated DNA fragment that contains the 3′ third of the UL52 ORF, the entire UL53 ORF, and a portion of the UL54 ORF (Fig. 2b). The probe hybridized to two wild-type KOS DNA fragments, the *Bam*HI L fragment (5.3 kbp), which contains the UL52 and UL53 ORFs, and the *Bam*HI B fragment (10.1 kbp), which contains the UL54 ORF (lane 5). As expected, the labeled probe hybridized to a single DNA fragment of ΔgK of approximately 14.4 kbp. This DNA fragment represented *Bam*HI-L plus *Bam*HI-B (5.3 kbp + 10.1 kbp = 15.4 kbp) minus the deletion in the gK gene (1.0 kbp). DNA sequencing revealed that the *Bam*HI site joining the *Bam*HI L and B DNA fragments was lost in the engineered gK deletion, resulting in the fusion of the *Bam*HI L and B DNA fragments (data not shown).

Rescue of the ΔgK virus by DNA fragments spanning the gK gene. To ascertain that the phenotype of the deletion mutant was due solely to the deletion of the gK gene, marker rescue experiments were performed with DNA fragments that spanned the entire gK gene. Primers P1 and P4 were used to generate a 3.9-kbp PCR fragment, using KOS viral DNA as the template. The PCR-amplified DNA fragment was transfected into Vero cells, and 24 h posttransfection, cells were infected with ΔgK virus. Cell cultures were incubated at 37°C for an additional 48 h, at which point virus stocks were prepared. Recombinant virus stocks were plated on subconfluent Vero cell monolayers (8×10^5 cells per 9.62 cm^2 at the time of infection) at different dilutions and allowed to replicate for 48 h. At 48 hpi, plaque morphologies were assessed in a phase-contrast microscope. Approximately 4% of the plaques appeared larger than the typical small plaques produced by the ΔgK virus. A typical virus plaque produced by the ΔgK revertant virus, designated ΔgK^+, is shown in Fig. 3B. Virus stocks were prepared from four different large plaques and plaque purified three times. The DNA from these plaques was extracted and subjected to diagnostic PCR. All four viral DNAs were positive for the presence of the entire gK gene and indistinguishable from the wild-type KOS genotype.

Rescue efficiency of KOS (*d*27-1) virus by plasmids pSJ1763 and pSJ1724, carrying the ΔgK and F-gKβ gK gene deletions, respectively. To ascertain whether the observed phenotypic properties of F-gKβ were due to the truncated gK expressed by F-gKβ, experiments were performed to produce a recombinant KOS virus with the F-gKβ gK gene. Different amounts of plasmids pSJ1724 and pSJ1763 were transfected into Vero cells and subsequently superinfected with *d*27-1 virus. Stocks of viruses were prepared at 24 hpi and titered onto Vero and VK302 cells. Plasmid pSJ1724 (1 μg) containing the ΔgK deletion produced 40-fold more virus on Vero cells than pSJ1763 (1 μg) and approximately 7-fold more virus at a plasmid concentration of 5 μg (Table 1). Twenty-five individual plaques were collected from each transfection, viruses were plaque purified twice, and individual plaques were tested by PCR analysis to identify recombinant viruses that contained either the ΔgK or F-gKβ allele. Transfections with plasmid pSJ1763 failed to produce a recombinant virus that contained the F-gKβ gK gene, while transfections with pSJ1724 produced six recombinant viruses with the gK deletion (not shown).

Plaque morphologies of ΔgK and F-gKβ mutant viruses on Vero and VK302 cells. The ΔgK virus was plated on exponentially growing Vero and VK302 cells containing approximately 8×10^5 cells per 9.62-cm^2 well of a six-well plate, and the resultant viral plaques were examined microscopically 3 days postinfection. ΔgK formed smaller plaques on Vero cells than the wild-type KOS virus (Fig. 3A and C). The wild-type KOS and revertant ΔgK^+ plaques formed on VK302 cells were similar to those obtained on Vero cells (Fig. 4A and B). ΔgK produced larger, nonsyncytial plaques on VK302 compared to Vero cells; however, these viral plaques were smaller than KOS or ΔgK^+ viral plaques, suggesting that ΔgK was not fully complemented by VK302 cells (Fig. 4C). F-gKβ produced partially syncytial, large plaques on VK302 cells (Fig. 4D).

The effect of Melittin on F-gKβ-induced cell fusion of 143TK$^-$ cells. Monolayers of 143TK$^-$ cells were infected with either ΔgK or F-gKβ at an MOI of 1. The morphological appearance of infected cells was examined at 24 hpi in a phase-contrast microscope. F-gKβ-induced extensive cell fusion of 143TK$^-$ cells, in contrast with ΔgK, which did not cause cell fusion of 143TK$^-$ cells (Fig. 5A, C, and E). Melittin, a specific inhibitor of gK-mediated virus-induced cell fusion (4), inhibited F-gKβ and MP-induced cell fusion of 143TK$^-$ cells effectively (Fig. 5D and F).

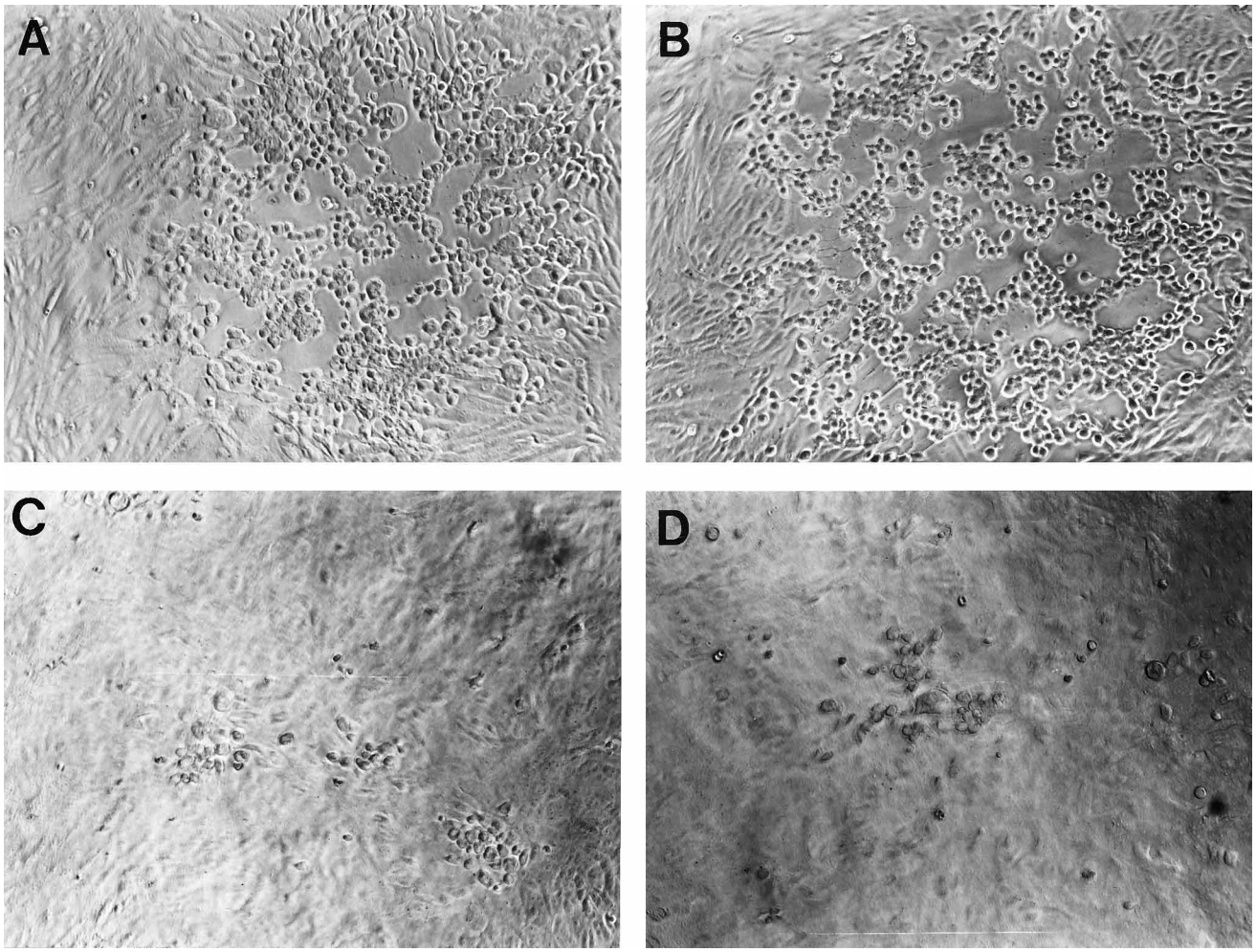

FIG. 3. Plaque morphologies of KOS (A), ΔgK$^+$ (B), ΔgK (C), and F-gKβ (D) viruses on Vero cells. Cells were infected at an MOI of 0.2 PFU/cell and photographed through a phase-contrast microscope at 72 hpi.

Propagation and plaquing efficiencies of ΔgK and F-gKβ on Vero and VK302 cells. Equal numbers of infectious virions obtained by titration on actively dividing Vero and VK302 cells for ΔgK and F-gKβ, respectively, were used to infect Vero and VK302 cells at an MOI of 2. Virus stocks were collected at 24 hpi, and titers were determined on log-phase Vero and VK302 cells. The results of these experiments are shown in Tables 2 and 3. The plaquing efficiency of ΔgK virus in actively replicating Vero cells was approximately 100,000-fold higher than in stationary-phase Vero cells. By contrast, the plaquing efficiency of F-gKβ was 60-fold higher in actively replicating than stationary Vero cells (Table 2). ΔgK and F-gKβ virus stocks prepared in the complementing cell line VK302 produced approximately equal numbers of viral plaques on VK302 cells. However, when titers of these viral stocks were determined on log-phase Vero cells, the number of viral plaques produced by F-gKβ virus was approximately 3,000-fold lower than the number of ΔgK viral plaques (Table 3). Moreover, F-gKβ virus stocks prepared in Vero cells produced 16,000-fold less viral plaques on actively replicating cells than ΔgK virus stocks (Table 2). The plaquing efficiency of KOS virus stocks prepared in VK302 cells was reduced 10-fold in actively replicating VK302 cells in comparison to Vero cells.

TABLE 1. Marker rescue frequencies[a]

Plasmid and concn (μg)	Titer (PFU/ml) on:	
	Vero cells	VK302 cells
pSJ1763 (1)	3.67 ± 1.15	7.0 ± 1.0
pSJ1763 (5)	62.67 ± 3.1	86.67 ± 4.73
pSJ1724 (1)	113 ± 15	102 ± 10
pSJ1724 (5)	386 ± 10.3	425 ± 25

[a] Vero cells were transfected with either pSJ1693 or pSJ1724 and 18 h post-transfection were infected with the *d*27-1 virus at an MOI of 10. Virus stocks were collected at 24 hpi and their titers were obtained by serial dilution on the indicated cell lines. Results represent the averages of three different experiments.

Kinetics of ΔgK and F-gKβ infectious virus production. The kinetics of ΔgK infectious virus production was examined by measuring the number of PFU at different times after infection. Equal numbers of subconfluent Vero and HEp-2 cells (8×10^5 cells per 9.62 cm^2 at the time of infection) were infected with mutant ΔgK and the wild-type KOS virus, respectively, at a MOI of 10. Virus stocks were prepared from cellular extracts and from the supernatant fluids of infected cell cultures. The infectious virus production kinetics of intracellular ΔgK on Vero cells was markedly different from that of the

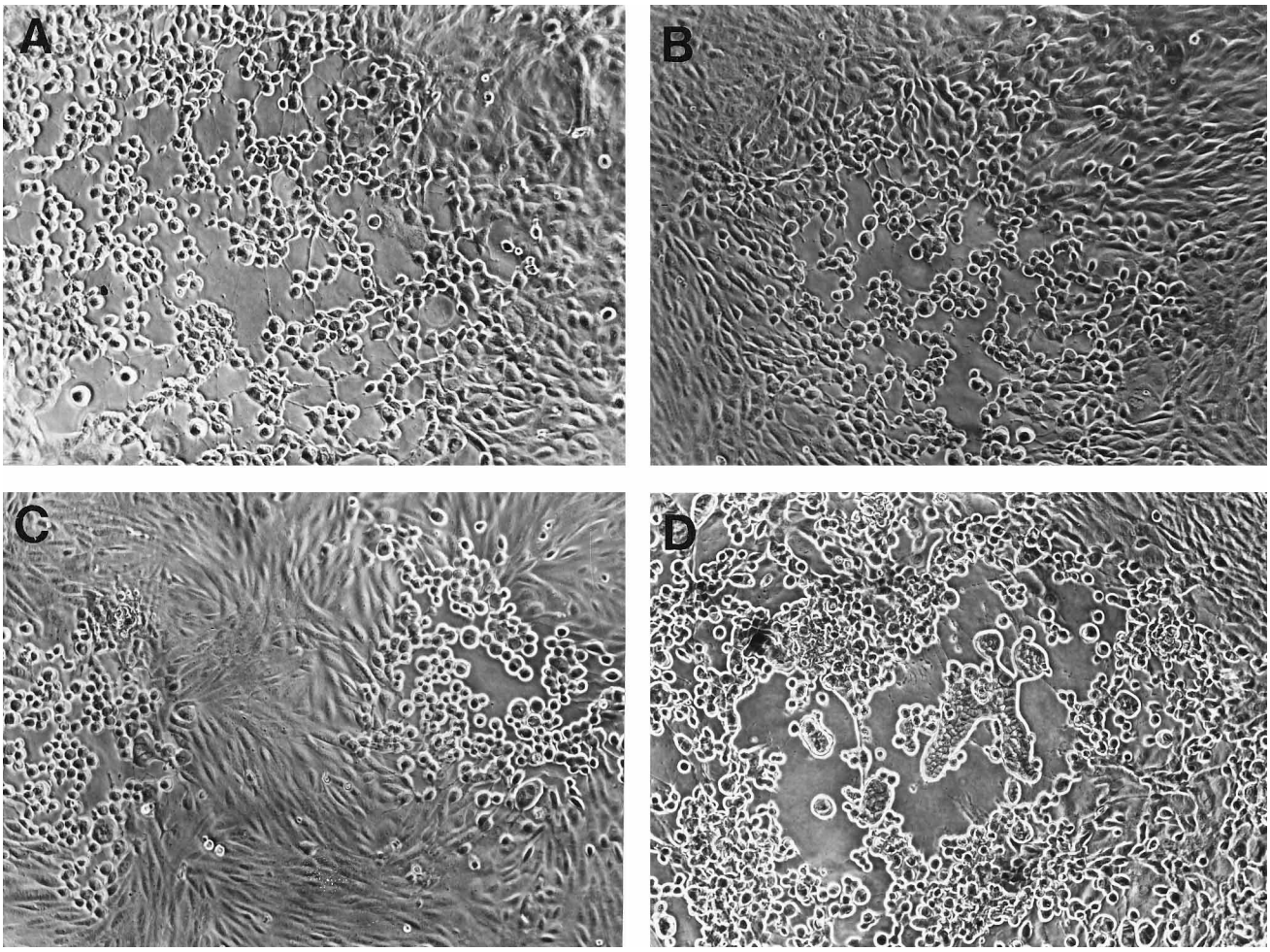

FIG. 4. Plaque morphologies of KOS (A), ΔgK^+ (B), ΔgK (C), and F-gKβ (D) viruses on VK302 cells. Cells were infected at an MOI of 0.2 PFU/cell and photographed through a phase-contrast microscope at 72 hpi.

corresponding wild-type KOS virus, and the maximum number of intracellular infectious virions was 400-fold lower than that of KOS in Vero cells (Fig. 6A). By contrast, the maximum number of intracellular ΔgK virions was 10-fold less than that of KOS in HEp-2 cells (Fig. 6B). The ratios of maximum intracellular to extracellular virus on Vero cells were approximately 1 for KOS and 500,000 for ΔgK; on HEp-2 cells, these ratios were 2 for KOS and 500,000 for ΔgK (Fig. 6A and B).

A side-by-side comparison of the growth kinetics of ΔgK and F-gKβ viruses was performed (Fig. 6C). ΔgK stocks were propagated in Vero cells, and titers were determined by serial dilution in Vero cells; F-gKβ virus stocks were prepared in

TABLE 2. Plaquing efficiencies of viruses grown on Vero cells[a]

Virus	Titer determined on:	Genotype	Phenotype	Titer (PFU/ml)	
				Stationary-phase cells	Log-phase cells
KOS	Vero	gK^+	gK^+ syn^+	5.5×10^9	1.8×10^{10}
	VK302	gK^+	gK^+ syn^+	7.7×10^9	8.0×10^9
ΔgK	Vero	ΔgK	ΔgK syn^+	3.2×10^3	2.9×10^8
	VK302	ΔgK	ΔgK syn^+	7.7×10^7	7.1×10^7
F-gKβ	Vero	gKβ	gKβ syn	3×10^2	1.8×10^4
	VK302	gKβ	gKβ syn	6.5×10^5	4.5×10^7

[a] Virus stocks were prepared by infecting Vero cells at an MOI of 2. Infected cells and supernatant fluids were collected and combined at 24 hpi. The relative plaquing efficiencies of virus stocks were determined by serial dilution on Vero cells. Results represent averages of three independent experiments in which three culture chambers of a six-chamber plastic dish were infected in parallel. Individual titers varied less than twofold among the different experiments. Each cell culture well (9.62 cm^2) contained approximately 2.5×10^6 cells at stationary phase and 8×10^5 cells per 9.62 cm^2 well at log phase at the time of exposure to viruses.

TABLE 3. Plaquing efficiencies of viruses grown on VK302 cells[a]

Virus	Titer determined on:	Genotype	Phenotype	Titer	
				PFU/ml	Relative to KOS titer
KOS	Vero	gK^+	gK^+ syn^+	6×10^{10}	11
	VK302	gK^+	gK^+ syn^+	5.1×10^9	1
ΔgK	Vero	ΔgK	ΔgK syn^+	1.3×10^9	0.25
	VK302	ΔgK	ΔgK syn^+	6×10^9	1.17
F-gKβ	Vero	gKβ	gKβ syn	4.5×10^5	0.00008
	VK302	gKβ	gKβ syn	7×10^9	1.37

[a] Virus stocks were prepared by infecting VK302 cells at an MOI of 2. For other details, see the footnote to Table 2.

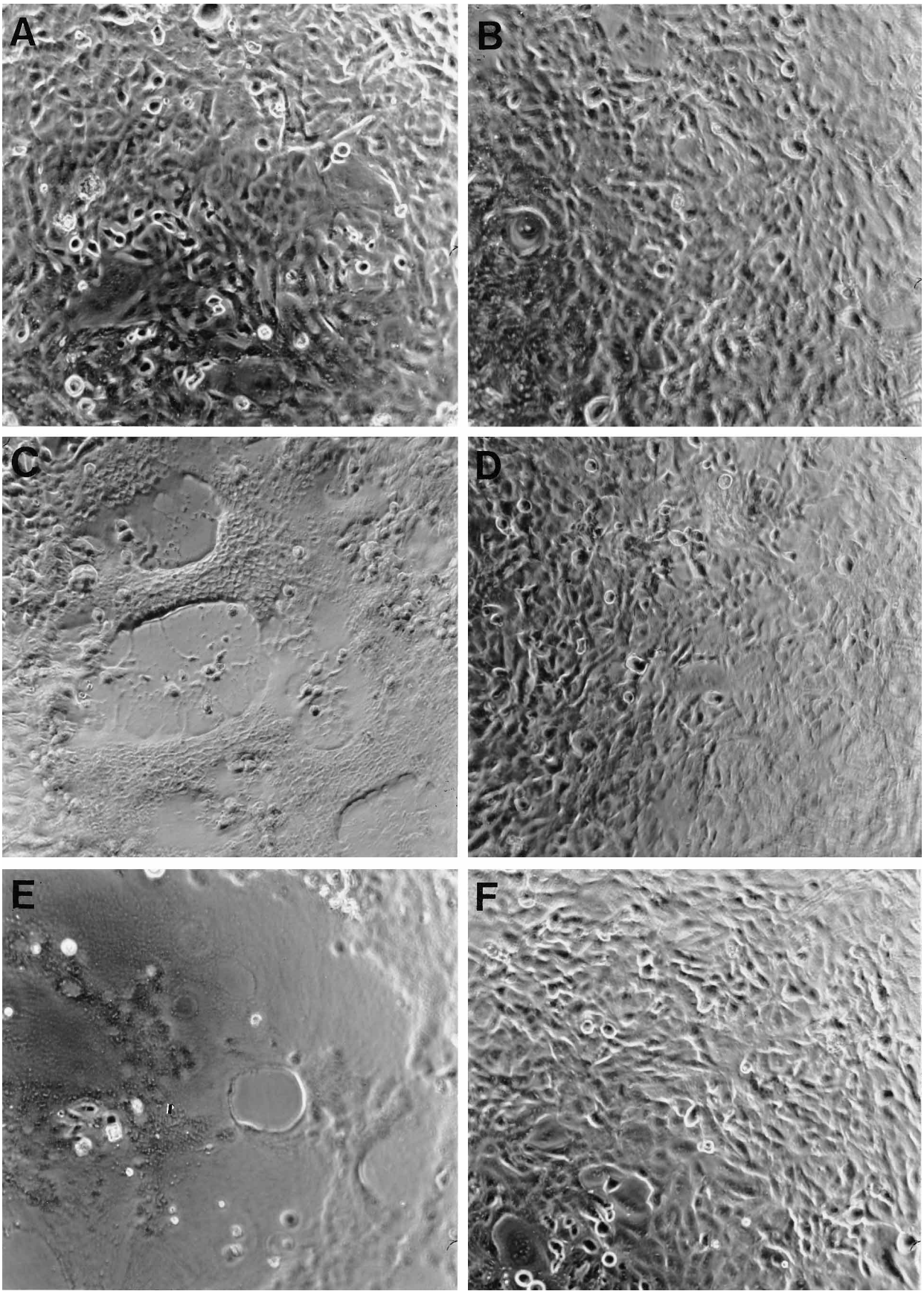

FIG. 5. Effect of melittin on F-gKβ and MP-induced fusion of 143TK$^-$ cells. Subconfluent 143TK$^-$ cells were infected with either ΔgK (A and B), F-gKβ (C and D), or MP (E and F) at an MOI of 1. Melittin was added immediately after adsorption of the viruses at a concentration of 0.75 μM (B, D, and F). Infected cells cultures were photographed at 24 hpi, using a phase-contrast microscope.

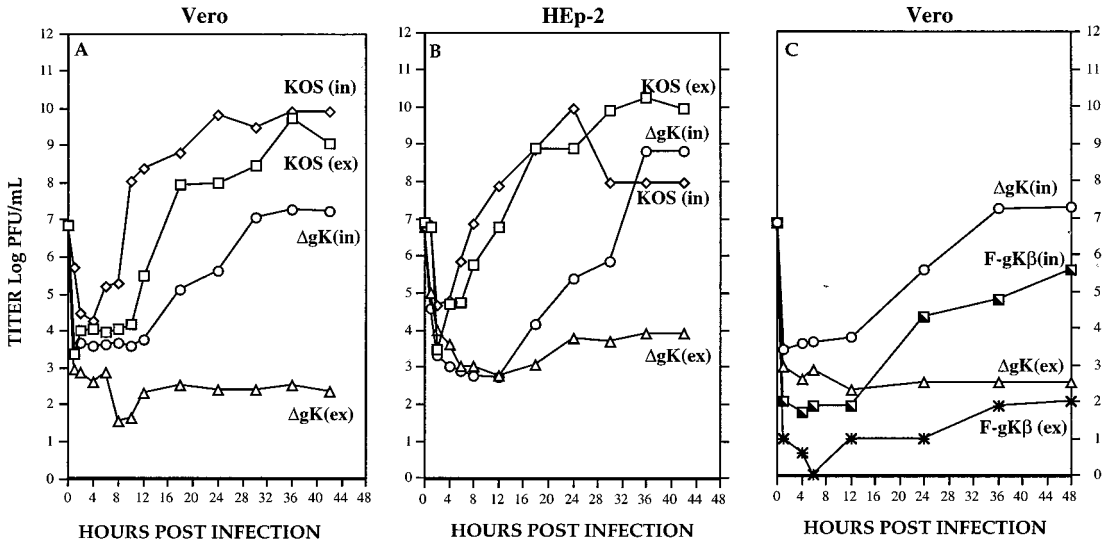

FIG. 6. Kinetics of infectious virus production. Subconfluent Vero and HEp-2 cells containing approximately 8×10^5 cells per 9.62 cm^2 at the time of infection (A and B) were infected at an MOI of 10 with KOS and ΔgK viruses, respectively. Subconfluent Vero cells (C) were infected at an MOI of 10 with either ΔgK or F-gKβ virus. At various times after infection, virus stocks were prepared from the supernatants and cell extracts, and titers were determined on Vero cells. (ex), extracellular; (in), intracellular.

VK302 cells, and titers were determined in VK302 cells. Equal numbers of infectious virions were used to infect subconfluent Vero cell monolayers at an MOI of 10, and the amounts of virus produced at different times were assessed by serial dilutions of virus stocks in Vero for ΔgK and VK302 for F-gKβ. In this comparison, ΔgK produced approximately 50-fold more infectious virions than F-gKβ at 48 hpi. Infectious ΔgK and F-gKβ viruses accumulated exclusively within infected cells, while only a small fraction of the total number of infectious virions were found in the extracellular fluids (Fig. 6C).

Electron microscopy. Conventional fixation-embedding electron microscopic analysis was undertaken to identify the intracellular localization of ΔgK virus in Vero and HEp-2 cells. Intracellular virus was examined only in cells with morphologically intact nuclear membranes to avoid studying late secondary cytocidal effects. The nuclei of all cells viewed at 72 hpi appeared normal, exhibiting margination of the chromatin along the nuclear membrane, indicating that there was no destruction of nuclear structures. In Vero cells infected with ΔgK, at 72 hpi there was an accumulation of capsids in the nucleus appearing in paracrystalline arrays proximal to the nuclear membrane (Fig. 7A), and enveloped capsids were visualized in the cytoplasm (Fig. 7B). In contrast, enveloped virus particles were detected in the cytoplasm and extracellular spaces of KOS-infected Vero cells (Fig. 7C and D). Electron micrographs of ΔgK-infected HEp-2 cells revealed capsids in the nuclei of infected cells, while enveloped virions were visualized in the cytoplasm as either enveloped virions, free capsids, or clusters of capsids enclosed within vesicles (Fig. 7E and F).

Characterization of ΔgK-specified glycoprotein synthesis and transport to the cell surface. To ascertain the relative amounts of gB, gC, gD, and gH on the surface of KOS- and ΔgK-infected cells, subconfluent Vero cell cultures were infected with either KOS or ΔgK virus at an MOI of 5, and the expression of gB, gC, gD, and gH was examined by fluorescence cytometry. Approximately equivalent amounts of all four glycoproteins were synthesized and transported to the surface of either KOS- or ΔgK-infected cells (Fig. 8).

DISCUSSION

Insertional inactivation of the HSV-1 (F) gK gene led to the conclusion that gK is essential for virus replication in cell culture, because the resultant recombinant virus F-gKβ was unable to replicate in cell culture (28). In this report, we substantially extended previous findings by producing and characterizing the gK-null virus ΔgK with a deletion of the entire gK gene coding for the mature gK. The phenotypic properties of ΔgK in infected cell cultures revealed that (i) gK is not essential for virus replication in exponentially dividing cells, (ii) gK is essential for the translocation of infectious virions from the cytoplasm to the extracellular spaces, and (iii) the syncytial phenotype and the reduced plaquing efficiency and replication ability of F-gKβ in Vero cells by comparison to ΔgK are most likely due to the expression of the amino-terminal portion of gK.

Role of gK in virus envelopment. Exponentially dividing Vero cells produced substantially more infectious ΔgK virions than stationary Vero cells but 10-fold less than HEp-2 cells. Furthermore, infectious ΔgK virions failed to translocate to extracellular spaces. These results indicate that actively replicating Vero cells and HEp-2 cells most likely complemented the ΔgK-null defect for virus envelopment. HEp-2 cells are transformed cells originally isolated from a human epidermoid larynx carcinoma (37). In cell culture, HEp-2 cells remain metabolically active even at nearly 100% confluency, as evidenced by the fact that they incorporated [^{35}S]methionine into their proteins (15) and [^{3}H]thymidine into their DNA (unpublished observations). gK has been detected exclusively on the surface of nuclei and ER membranes by using anti-gK antibodies (29). We hypothesize that nuclear membranes of dividing cells may complement the absence of gK because they are primed for mitotic division. In this hypothesis, gK may cause nuclear membrane reorganization events to increase the efficiency of virus envelopment. Cellular complementation by exponentially growing cells was also reported for the HSV-1 strain 17 syn$^+$ ICP34.5 gene, which codes for a viral tegument protein, γ34.5. Deletion of the ICP34.5 (γ34.5) viral gene in

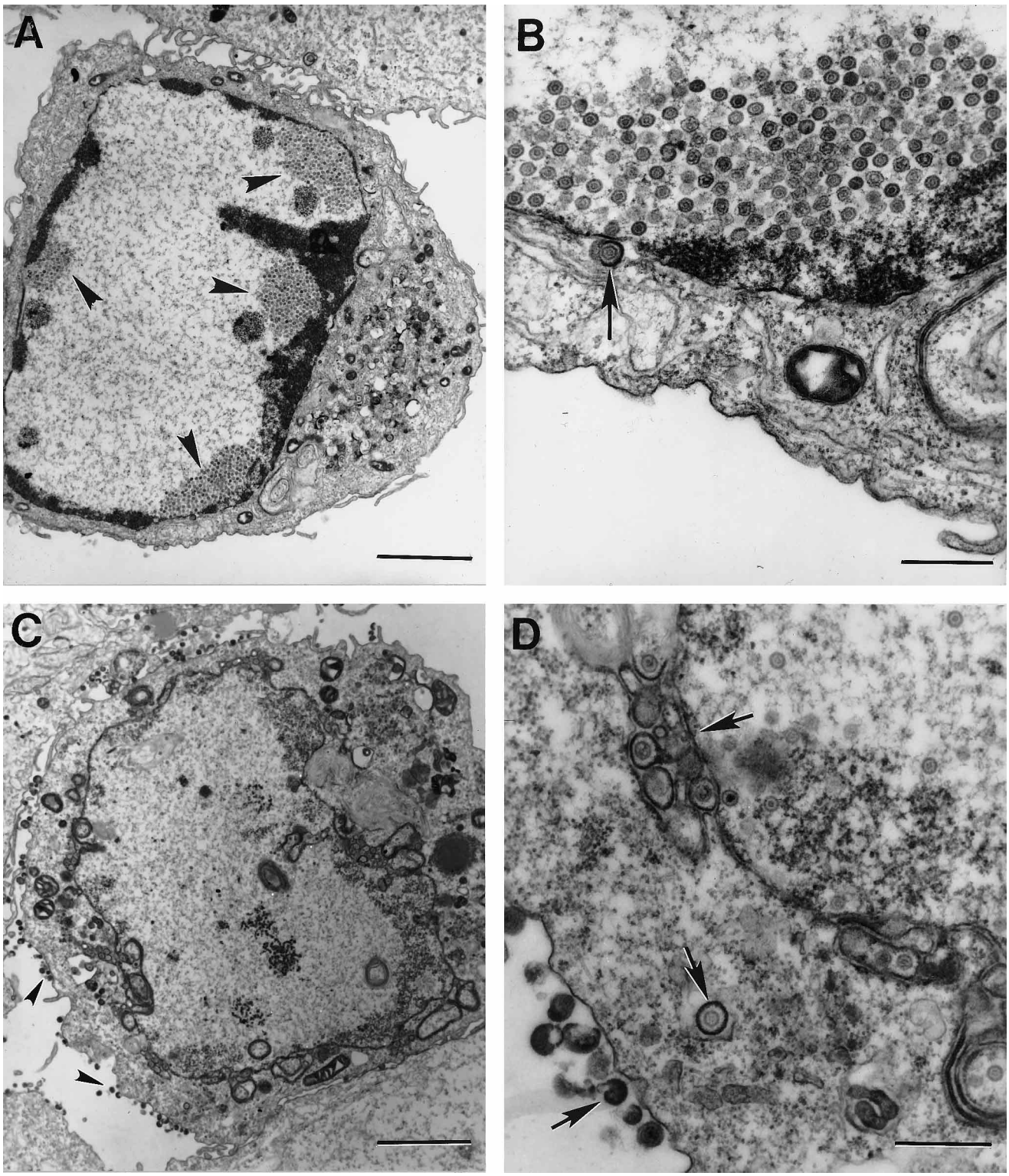

FIG. 7. Electron micrographs of Vero and HEp-2 cells infected with ΔgK and KOS viruses. Subconfluent Vero cells were infected with ΔgK virus (A and B) and KOS virus (C and D), and HEp-2 cells were infected with ΔgK virus (E and F). All cells were infected at an MOI of 10 PFU/cell, incubated at 37°C for 72 h, and prepared for electron microscopy. The arrowheads in panel A point to arrays of viral capsids in the nucleus. The arrow in panel B point to an enveloped ΔgK virus in the cytoplasm. Arrowheads in panel C mark the extracellular KOS virus. Arrows in panel D point to KOS virions in the perinuclear space, cytoplasm, and extracellular space. In panel E, the arrows mark enveloped virions in the cytoplasm; in panel F, the arrowheads mark ΔgK nucleocapsids found in cytoplasmic vesicles. n, nucleus; c, cytoplasm; e, extracellular space. Scale bars = 0.5 μm.

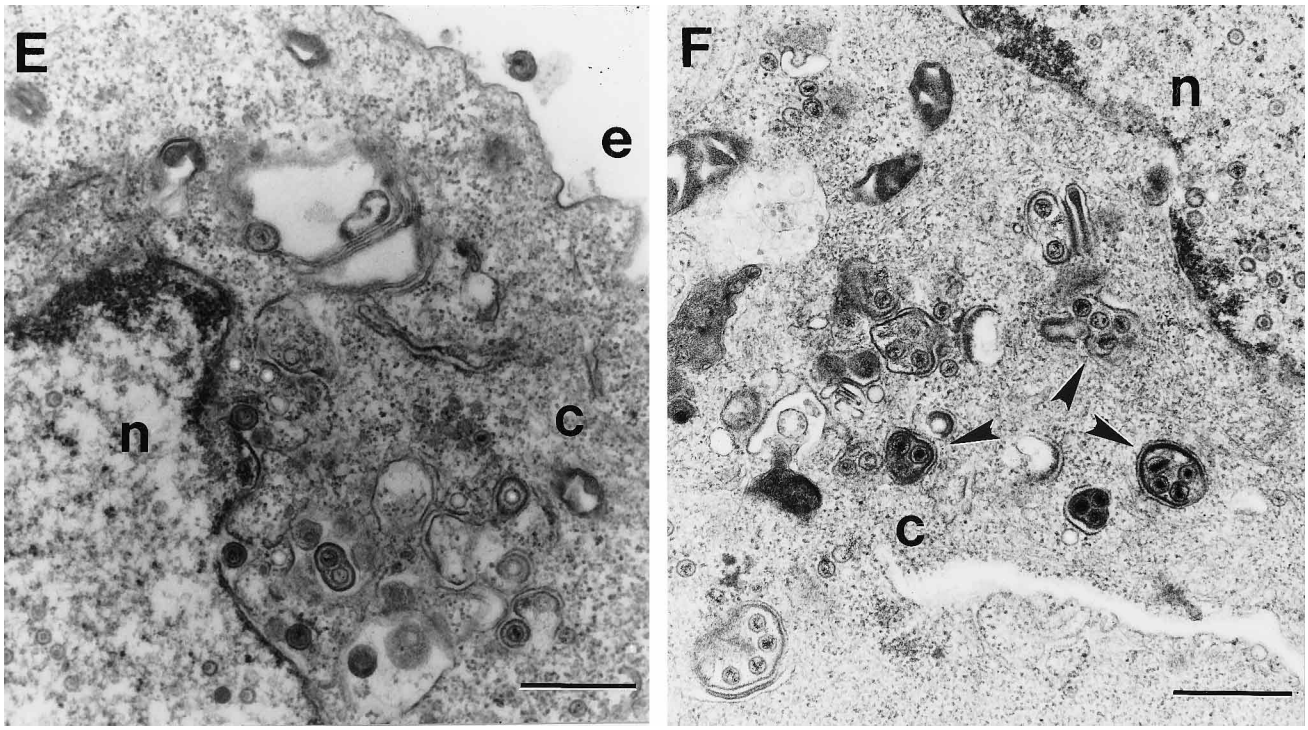

FIG. 7—*Continued.*

HSV-1 strain 17 syn$^+$ resulted in virions that failed to envelope, while capsids accumulated in the nuclei of infected stationary-phase 3T6 cells. However, the ICP34.5 null virus replicated efficiently in log-phase 3T6 cells (10).

Role of gK in the translocation of infectious virions from the cytoplasm to the extracellular space. Infectious ΔgK virions accumulated within the cytoplasm of Vero and HEp-2 cells, indicating that gK plays an important role in release of cytoplasmic virions to the extracellular spaces. A similar retention of infectious virions within cells was noted when Golgi-specified enzymatic functions were inhibited either by Golgi-specific inhibitors or in mutant cells deficient in specific Golgi-localized enzymes, indicating that the Golgi apparatus is important in virion egress (7, 16, 31). Previous studies indicated that gK contains high-mannose carbohydrate moieties which are characteristic of the RER, and indirect immunofluorescence with antipeptide antibodies failed to detect gK in the cytoplasm of infected cells (28, 29). Glycoprotein synthesis and expression on the surface of ΔgK-infected cells were similar to those of KOS-infected cells, indicating that the Golgi apparatus functioned properly and that glycoprotein synthesis and cell surface expression of glycoproteins are independent of virion egress. Therefore, these results suggest that gK does not inhibit virion egress by inhibiting Golgi-dependent functions.

Previous studies showed that HSV-1 (KOS) virions containing high-mannose glycoproteins derived from the RER were fully infectious (32). We favor the hypothesis that the envelopes of ΔgK virions found in the cytoplasm of ΔgK-infected cells originated from the outer lamellae of the nuclear membrane and that the absence of gK causes an inhibition of transport of enveloped virions to the Golgi apparatus, where further maturation of glycoproteins would occur. Alternatively, the presence of fully glycosylated glycoproteins in the envelopes of cytoplasmic ΔgK virions suggests that the absence of gK inhibits a post-Golgi virion egress step. Characterization of the viral glycoproteins incorporated in ΔgK virions should resolve the origin of ΔgK virion envelopes.

There are obvious similarities in virion transport defects caused by mutations in UL20, gH, and gK which imply that these three proteins may share some functions in intracellular virion transport. However, ΔgK virus is not complemented in many cell lines, including the 143TK$^-$ cell line, which complements the UL20-null virus, implying that there are important differences between gK and UL20 functions. Mutant viruses that carry a temperature-sensitive mutation in gH synthesize at the nonpermissive temperature immature gH which is not transported to the cell surface, and infectious virions accumulate in the cytoplasm (28). In contrast, gH is synthesized and expressed at the cell surface of ΔgK-infected cells, implying that gK's role in virion transport is different from that of gH.

Molecular basis for the genotypic and phenotypic differences between ΔgK and F-gKβ viruses. The genotypes of F-gKβ and ΔgK mutant viruses are distinct. F-gKβ was created by insertional inactivation of the gK gene by using an ICP6::*lacZ* cassette. This insertion allowed for the expression of the first 112 amino acids of gK fused to 26 amino acids originating from the 5′-most DNA sequence of the ICP6 promoter of the ICP6::*lacZ* gene cassette (26, 28). The extra 26 amino acids that are fused to the amino-terminal 112 amino acids of gK are DPRARRFCTWYSLTASAGTRSCVVCT (26a). This amino acid sequence was also independently predicted in our laboratory from the complete ICP6::*lacZ* DNA sequence (55) (not shown). It was hypothesized that this fusion protein is degraded because it does not contain the hydrophobic portion of gK that is thought to anchor gK to membranes. Furthermore, it was not possible to detect this truncated gK in F-gKβ-infected cells (28). Interestingly, this 112-amino-acid sequence contains the Syn1 locus that demarcates the putative fusion domain of gK (24).

Side-by-side comparisons of the replication and plaquing

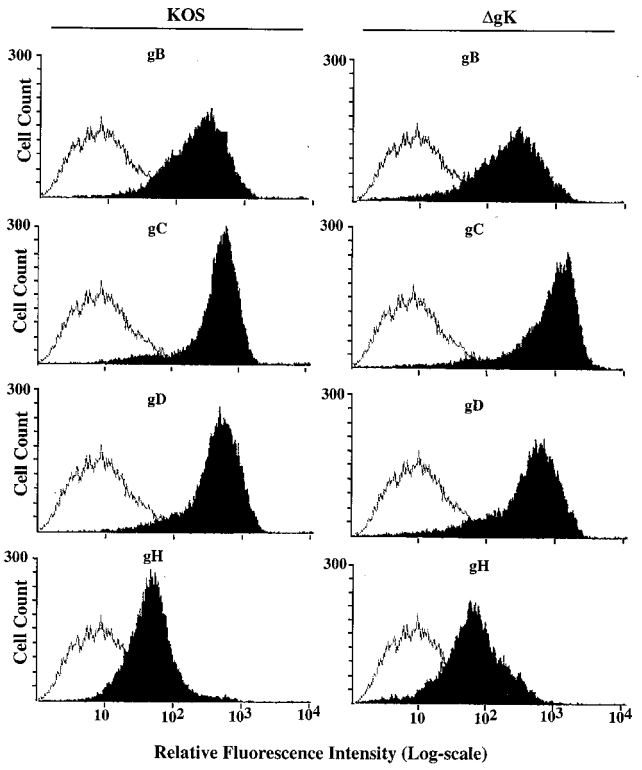

FIG. 8. Fluorescence cytometry profiles of KOS and ΔgK-infected Vero cells obtained by using MAbs to gB, gC, gD, and gH and goat anti-mouse antibody conjugated to FITC. Background measurements were determined by staining infected control cells immediately after adsorption of the virus (0 hpi).

efficiencies of ΔgK and F-gKβ mutant viruses on different cell lines revealed substantial differences. First, F-gKβ caused cell fusion of 143TK$^-$ cells and limited fusion of gK-transformed cells VK302, while ΔgK did not cause cell fusion of either 143TK$^-$ or VK302 cells. Importantly, the cell fusion caused by F-gKβ was sensitive to melittin, a specific inhibitor of gK-induced cell fusion (4), indicating that the truncated gK specified by F-gKβ is responsible for the F-gKβ syncytial phenotype. Second, the F-gKβ plaquing efficiency on Vero cells was drastically reduced in comparison to that of ΔgK, while the plaquing efficiencies of both viruses on the complementing cell line VK302 were nearly identical. Moreover, one-step virus replication experiments indicated that F-gKβ virus replicated approximately 100-fold less efficiently than ΔgK virus in Vero cells. In general, syncytial mutants do not replicate as efficiently as nonsyncytial parental viruses; thus, part of the replication deficiency of F-gKβ may be due to its syncytial phenotype. Third, a recombinant plasmid which carried a 618-bp DNA fragment coding for the F-gKβ gene truncation failed to rescue the *d*27-1 virus, while a similar plasmid that carried the ΔgK gene deletion rescued *d*27-1 efficiently. Theoretically, the plasmid with the gK gene of F-gKβ should rescue *d*27-1 more efficiently than the plasmid with the ΔgK gene deletion due to the presence of the additional 618 bp of homologous DNA sequences at the 5′ end of the DNA construct. Moreover, recombinant viruses which carried the F-gKβ gK gene could not be isolated. HSV-1 (F) is a clinical strain which has been passed a limited number of times in cell culture, while KOS is a laboratory strain that has been passed a large number of times in cell culture. Furthermore, HSV-1 (F) specifies gB that contains the fast-entry genotype which enables HSV-1 (F) to enter cells faster than KOS (12, 41). This replication advantage and possibly other differences between these two viruses may enable F-gKβ to replicate at low levels in the presence of the gK truncation, while the same truncated gK may cause greater inhibition of virus replication in the context of the KOS than the F genomic background. These results suggest that the gK truncation is the principal cause of the reduced virus replication, plaquing efficiency, and syncytial phenotype of F-gKβ virus in comparison to ΔgK virus.

The viral yields of the one-step replication experiments were substantially reduced in comparison to viral yields in the plaquing efficiency experiments; however, in the one-step kinetics of replication and the plaquing efficiency experiments, ΔgK virus yields were substantially higher than F-gKβ virus yields (7- and 50-fold, respectively). Differences in the maximum viral yields attained between these two experiments may be partly due to the use of different MOIs, differences in the relative confluency of cells which were used to determine virus titers, and the relative instability of both gK-null virus stocks to freeze-thawing. Furthermore, the one-step virus replication experiments were performed by adsorbing viruses at 4°C for 1 h prior to incubation at 37°C, while plaquing efficiency experiments were performed by attaching viruses at 25°C for 1 h prior to incubation at 37°C. Therefore, the observed discrepancy of viral yields between the two types of experiments may be due to inefficient attachment and/or subsequent entry of F-gKβ and ΔgK viruses into Vero cells after attachment at 4°C. Additional experimentation is needed to clarify the role of gK in virus assembly, stability, attachment, and entry into cells.

Electron microscopic examination of Vero cells infected with F-gKβ virus showed that F-gKβ enveloped virions were predominantly found in the perinuclear space, and numerous capsids were also detected in the cytoplasm (28). On the basis of these findings, it was suggested that gK may prevent fusion between viral and cellular membranes, so that the virion particles do not lose their viral envelopes during intracellular transport. The cytoplasm of ΔgK-infected Vero cells contained either enveloped virions or a proportionally lower number of capsids without envelopes. ΔgK-infected HEp-2 cells contained, in addition to enveloped virions and capsids, multiple capsids enclosed within vesicles which appear to be derived by fusion of multiple viral envelopes, because they contained an electron-dense area immediately underneath the vesicle membrane similar to the tegument area of enveloped virion particles. Free capsids and capsids within these cytoplasmic vesicles may be due to nonspecific fusion among ΔgK virions with the exception that the resultant fusion vesicle is more stable in HEp-2 cells than in Vero cells. In this regard, the lower production of infectious virions in the cytoplasm of F-gKβ-infected cells (28) may be due to the membrane fusion properties of the truncated gK specified by F-gKβ, which may cause efficient loss of viral envelopes and accumulation of capsids in the cytoplasm of F-gKβ-infected cells.

Original descriptions of the syncytial phenotype attributed to the gK gene included the hypothesis that gK played the role of membrane fusion inhibitor or modulator of virus-induced cell fusion. Thus, a gK-null virus would be expected to cause syncytial plaques (34, 36, 44, 47, 52). Apparently, this hypothesis is not entirely correct, because ΔgK virions do not form syncytial plaques. However, the absence of gK may cause fusion among ΔgK viral envelopes in the cytoplasm of ΔgK-infected cells, which supports the role of gK as a membrane fusion inhibitor. The new role of gK in virion cellular egress suggests that there is a link between virion egress and virus-induced cell fusion. Elucidation of gK structure and function remains a crucial target in our quest to understand the role of

membrane fusion in herpesvirus assembly intracellular virion transport and egress as well as in the ever-elusive virus-induced cell-to-cell fusion mechanisms. In this regard, the availability of the ΔgK mutant virus in conjunction with already developed methods for gK gene site-directed mutagenesis (19) will facilitate further gK structure and function studies and the delineation of the functional domains of gK.

ACKNOWLEDGMENTS

We acknowledge the expert technical assistance of Laura Younger with electron microscopy and Marilyn Dietrich with fluorescence-activated cell sorting analysis. We are indebted to D. C. Johnson, L. Hutchinson, and D. M. Knipe for materials used in this study. We also thank S. Person, P. Spear, and L. Hutchinson for many helpful comments.

This work was supported in part by Public Health Service grant AI27886 to K.G.K., by NIH-IDea grant P20RR10230-01 for partly supporting S.J., and by support from the School of Veterinary Medicine, Louisiana State University, Baton Rouge.

REFERENCES

1. **Avitabile, E., G. S. Di, M. R. Torrisi, P. L. Ward, B. Roizman, and G. Campadelli-Fiume.** 1995. Redistribution of microtubules and Golgi apparatus in herpes simplex virus-infected cells and their role in viral exocytosis. J. Virol. **69:**7472–7482.
2. **Baghian, A., M. A. Dietrich, and K. G. Kousoulas.** 1992. Cell fusion caused by herpes simplex virus-1 (HSV-1) strains tsB5 and MP is inhibited at pH 6.7 and pH 7.0. Arch. Virol. **122:**119–131.
3. **Baghian, A., L. Huang, S. Newman, S. Jayachandra, and K. G. Kousoulas.** 1993. Truncation of the carboxy-terminal 28 amino acids of glycoprotein B specified by herpes simplex virus type 1 mutant *amb*1511-7 causes extensive cell fusion. J. Virol. **67:**2396–23401.
4. **Baghian, A., and K. G. Kousoulas.** 1993. Role of the Na^+, K^+ pump in herpes simplex type 1-induced cell fusion: melittin causes specific reversion of syncytial mutants with the syn1 mutation to Syn+ (wild-type) phenotype. Virology **196:**548–556.
5. **Baghian, A., L. Shaffer, and J. Storz.** 1990. Antibody response to epitopes of chlamydial major outer membrane proteins on infectious elementary bodies and of the reduced polyacrylamide gel electrophoresis-separated form. Infect. Immun. **58:**1379–1383.
6. **Baines, J. D., P. L. Ward, G. Campadelli-Fiume, and B. Roizman.** 1991. The UL20 gene of herpes simplex virus 1 encodes a function necessary for viral egress. J. Virol. **65:**6414–6424.
7. **Banfield, B. W., and F. Tufaro.** 1990. Herpes simplex virus particles are unable to traverse the secretory pathway in the mouse L-cell mutant *gro29*. J. Virol. **64:**5716–5729.
8. **Bond, V. C., and S. Person.** 1984. Fine structure physical map locations of alterations that affect cell fusion in herpes simplex virus type 1. Virology **132:**368–376.
9. **Bond, V. C., S. Person, and S. C. Warner.** 1982. The isolation and characterization of mutants of herpes simplex virus type 1 that induce cell fusion. J. Gen. Virol. **61:**245–254.
10. **Brown, S. M., A. R. MacLean, J. D. Aitken, and J. Harland.** 1994. ICP34.5 influences herpes simplex virus type 1 maturation and egress from infected cells in vitro. J. Gen. Virol. **75:**3679–3686.
11. **Browne, H., S. Bell, T. Minson, and D. W. Wilson.** 1996. An endoplasmic reticulum-retained herpes simplex virus glycoprotein H is absent from secreted virions: evidence for reenvelopment during egress. J. Virol. **70:**4311–4316.
12. **Bzik, D. J., B. A. Fox, N. A. DeLuca, and S. Person.** 1984. Nucleotide sequence of a region of the herpes simplex virus type 1 gB glycoprotein gene: mutations affecting rate of virus entry and cell fusion. Virology **137:**185–190.
13. **Bzik, D. J., B. A. Fox, N. A. DeLuca, and S. Person.** 1984. Nucleotide sequence specifying the glycoprotein gene, gB, of herpes simplex virus type 1. Virology **133:**301–314.
14. **Campadelli-Fiume, G., F. Farabegoli, G. S. Di, and B. Roizman.** 1991. Origin of unenveloped capsids in the cytoplasm of cells infected with herpes simplex virus 1. J. Virol. **65:**1589–1595.
15. **Campadelli-Fiume, G., M. T. Lombardo, L. Foa-Tomasi, E. Avitabile, and F. Serafini-Cessi.** 1988. Individual herpes simplex virus 1 glycoproteins display characteristic rates of maturation from precursor to mature form both in infected cells and in cells that constitutively express the glycoproteins. Virus Res. **10:**29–40.
16. **Campadelli-Fiume, G., S. Qi, E. Avitabile, L. Foa-Tomasi, R. Brandimarti, and B. Roizman.** 1990. Glycoprotein D of herpes simplex virus encodes a domain which precludes penetration of cells expressing the glycoprotein by superinfecting herpes simplex virus. J. Virol. **64:**6070–6079.
17. **Cavalcoli, J. D., A. Baghian, F. L. Homa, and K. G. Kousoulas.** 1993. Resolution of genotypic and phenotypic properties of herpes simplex virus type 1 temperature-sensitive mutant (KOS) tsZ47: evidence for allelic complementation in the UL28 gene. Virology **197:**23–34.
18. **Chen, C., and H. Okayama.** 1987. High-efficiency transformation of mammalian cells by plasmid DNA. Mol. Cell. Biol. **7:**2745–2752.
19. **Chouljenko, V., S. Jayachandra, G. Rybachuck, and K. G. Kousoulas.** 1996. Efficient long PCR site directed mutagenesis of a high GC-template. BioTechniques **21:**472–480.
20. **Compton, T., and R. J. Courtney.** 1984. Virus-specific glycoproteins associated with the nuclear fraction of herpes simplex virus type 1-infected cells. J. Virol. **49:**594–597.
21. **Darlington, R. W., and L. H. Moss III.** 1968. Herpesvirus envelopment. J. Virol. **2:**48–55.
22. **Debroy, C., N. Pederson, and S. Person.** 1985. Nucleotide sequence of a herpes simplex virus type 1 gene that causes cell fusion. Virology **145:**36–48.
23. **Desai, P. J., P. A. Schaffer, and A. C. Minson.** 1988. Excretion of noninfectious virus particles lacking glycoprotein H by a temperature-sensitive mutant of herpes simplex virus type 1: evidence that gH is essential for virion infectivity. J. Gen. Virol. **69:**1147–1156.
24. **Dolter, K. E., R. Ramaswamy, and T. C. Holland.** 1994. Syncytial mutations in the herpes simplex virus type 1 gK (UL53) gene occur in two distinct domains. J. Virol. **68:**8277–8281.
25. **Goldin, A. L., R. M. Sandri-Goldin, M. Levine, and J. C. Glorioso.** 1981. Cloning of herpes simplex virus type 1 sequences representing the whole genome. J. Virol. **38:**50–58.
26. **Goldstein, D. J., and S. K. Weller.** 1988. An ICP6::*lacZ* insertional mutagen is used to demonstrate that the UL52 gene of herpes simplex virus type 1 is required for virus growth and DNA synthesis. J. Virol. **62:**2970–2977.

26a. **Hutchinson, L.** Personal communication.

27. **Hutchinson, L., K. Goldsmith, D. Snoddy, H. Ghosh, F. L. Graham, and D. C. Johnson.** 1992. Identification and characterization of a novel herpes simplex virus glycoprotein, gK, involved in cell fusion. J. Virol. **66:**5603–5609.
28. **Hutchinson, L., and D. C. Johnson.** 1995. Herpes simplex virus glycoprotein K promotes egress of virus particles. J. Virol. **69:**5401–5413.
29. **Hutchinson, L., C. Roop-Beauchamp, and D. C. Johnson.** 1995. Herpes simplex virus glycoprotein K is known to influence fusion of infected cells, yet is not on the cell surface. J. Virol. **69:**4556–4563.
30. **Jacobson, J. G., S. L. Martin, and D. M. Coen.** 1989. A conserved open reading frame that overlaps the herpes simplex virus thymidine kinase gene is important for viral growth in cell culture. J. Virol. **63:**1839–1843.
31. **Johnson, D. C., and P. G. Spear.** 1982. Monensin inhibits the processing of herpes simplex virus glycoproteins, their transport to the cell surface, and the egress of virions from infected cells. J. Virol. **43:**1102–1112.
32. **Kousoulas, K. G., D. J. Bzik, and S. Person.** 1983. The effect of ammonium chloride and tunicamycin on the glycoprotein content and infectivity of herpes simplex virus type 1. Virology **125:**468–474.
33. **Kousoulas, K. G., P. E. Pellett, L. Pereira, and B. Roizman.** 1984. Mutations affecting conformation or sequence of neutralizing epitopes identified by reactivity of viable plaques segregate from syn and ts domains of HSV-1(F) gB gene. Virology **135:**379–394.
34. **Lee, G. T., and P. G. Spear.** 1980. Viral and cellular factors that influence cell fusion induced by herpes simplex virus. Virology **107:**402–414.
35. **MacLean, C. A., S. Efstathiou, M. L. Elliott, F. E. Jamieson, and D. J. McGeoch.** 1991. Investigation of herpes simplex virus type 1 genes encoding multiply inserted membrane proteins. J. Gen. Virol. **72:**897–906.
36. **Manservigi, R., P. G. Spear, and A. Buchan.** 1977. Cell fusion induced by herpes simplex virus is promoted and suppressed by different viral glycoproteins. Proc. Natl. Acad. Sci. USA **74:**3913–3917.
37. **Moore, A. E., L. Sabachewsky, and H. W. Toolan.** 1955. Culture characteristics of 4 permanent lines of human cancer cells. Cancer Res. **15:**598–602.
38. **Morgan, C., H. M. Rose, M. Holden, and E. P. Jones.** 1959. Electron microscopic observations on the development of herpes simplex virus. J. Exp. Med. **110:**643–656.
39. **Nii, S.** 1992. Electron microscopic study on the development of herpesviruses. J. Electron Microsc. **41:**414–423.
40. **Nii, S., C. Morgan, and H. M. Rose.** 1968. Electron microscopy of herpes simplex virus. II. Sequence of development. J. Virol. **2:**517–536.
41. **Pellett, P. E., K. G. Kousoulas, L. Pereira, and B. Roizman.** 1985. Anatomy of the herpes simplex virus 1 strain F glycoprotein B gene: primary sequence and predicted protein structure of the wild type and of monoclonal antibody-resistant mutants. J. Virol. **53:**243–253.
42. **Pogue-Geile, K. L., G. T. Lee, S. K. Shapira, and P. G. Spear.** 1984. Fine mapping of mutations in the fusion-inducing MP strain of herpes simplex virus type 1. Virology **136:**100–109.
43. **Pogue-Geile, K. L., and P. G. Spear.** 1987. The single base pair substitution responsible for the syn phenotype of herpes simplex virus type 1, strain MP. Virology **157:**67–74.
44. **Read, G. S., S. Person, and P. M. Keller.** 1980. Genetic studies of cell fusion induced by herpes simplex virus type 1. J. Virol. **35:**105–113.
45. **Rice, S. A., and D. M. Knipe.** 1990. Genetic evidence for two distinct transactivation functions of the herpes simplex virus alpha protein ICP27. J. Virol. **64:**1704–1715.

46. **Roizman, B., and A. E. Sears.** 1996. Herpes simplex viruses and their replication, p. 2231–2295. *In* B. N. Fields, D. M. Knipe, and P. M. Howley (ed.), Fields virology, 3rd ed., vol. 2. Lippincott-Raven Publishers, Philadelphia, Pa.
47. **Ruhlig, M. A., and S. Person.** 1977. Alterations of neutral glycolipids in cells infected with syncytium-producing mutants of herpes simplex virus type 1. J. Virol. **24:**602–608.
48. **Ryechan, W. T., L. S. Morse, D. M. Knipe, and B. Roizman.** 1979. Molecular genetics of herpes simplex virus. II. Mapping of the major viral glycoproteins and of the genetic loci specifying the social behavior of infected cells. J. Virol. **29:**677–697.
49. **Sanders, P. G., N. M. Wilkie, and A. J. Davison.** 1982. Thymidine kinase deletion mutants of herpes simplex virus type 1. J. Gen. Virol. **63:**277–295.
50. **Schwartz, J., and B. Roizman.** 1969. Concerning the egress of herpes simplex virus from infected cells: electron and light microscope observations. Virology **38:**42–49.
51. **Southern, E. M.** 1975. Detection of specific sequences among DNA fragments separated by gel electrophoresis. J. Mol. Biol. **98:**503–517.
52. **Spear, P. G.** 1993. Membrane fusion induced by herpes simplex virus, p. 201–232. *In* J. Bentz (ed.), Viral fusion mechanisms. CRC Press, Boca Raton, Fla.
53. **Stackpole, C. W.** 1969. Herpes-type virus of the frog renal adenocarcinoma. I. Virus development in tumor transplants maintained at low temperature. J. Virol. **4:**75–93.
54. **Ward, P. L., G. Campadelli-Fiume, E. Avitabile, and B. Roizman.** 1994. Localization and putative function of the UL20 membrane protein in cells infected with herpes simplex virus 1. J. Virol. **68:**7406–7417.
55. **Weeler, S.** Personal communication.
56. **Whealy, M. E., J. P. Card, R. P. Meade, A. K. Robbins, and L. W. Enquist.** 1991. Effect of brefeldin A on alphaherpesvirus membrane protein glycosylation and virus egress. J. Virol. **65:**1066–1081.